A method for geological hazard extraction using high-resolution remote sensing

Q J Wang[1], M X Li[2], Y Chen[1], J T Bi[1], Q Z Lin[1]
1 Key Laboratory of Digital Earth, Center for Earth Observation and Digital Earth, Chinese Academy of Sciences, No. 9 Deng Zhuang South Road, Haidian District, Beijing, China.
2 China Earthquake Networks Center, No. 5 Sanlihe Nanheng Street, Xicheng District, Beijing, China.

E–mail: wangqin08262002@yahoo.com.cn

Abstract. Taking Yingxiu, the epicentre of the Wenchuan earthquake, as the study area, a method for geological disaster extraction using high-resolution remote sensing imagery was proposed in this study. A high-resolution Digital Elevation Model (DEM) was used to create mask imagery to remove interfering factors such as buildings and water at low altitudes. Then, the mask imagery was diced into several small parts to reduce the large images' inconsistency, and they were used as the sources to be classified. After that, vector conversion was done on the classified imagery in ArcGIS. Finally, to ensure accuracy, other interfering factors such as buildings at high altitudes, bare land, and land covered by little vegetation were removed manually. Because the method can extract geological hazards in a short time, it is of great importance for decision-makers and rescuers who need to know the degree of damage in the disaster area, especially within 72 hours after an earthquake. Therefore, the method will play an important role in decision making, rescue, and disaster response planning.

1. Introduction

Macroscopic, real-time, objective remote sensing plays an important role in the assessment of earthquake damage. Wei C J [1] reviewed the history of the investigation and assessment of earthquake damage based on remote sensing in China, and drew the conclusion that remote sensing played an important role in the assessment of earthquake damage. Xu C [2] illustrated geological disasters such as landslips, landslides, and debris flows using remote sensing data. Chen W K [3] summarized the change detection methods of extracting earthquake disaster information from remote sensing imagery in China and elsewhere in recent years. Wang X Q [4] discussed progress in earthquake damage extraction studies using remote sensing imagery. Wang X Q [5] introduced essential quantitative study methods, the concept of the remote sensing seismic damage index, and analysis models. The results suggested that quantitative studies on seismic damage based on remote sensing could provide an effective method for seismic damage surveying and loss estimation. Cai S [6] mapped seismic intensity distribution on the basis of the Chinese seismic intensity scale by analysing damage to buildings, roads, bridges, and geological disasters induced by earthquakes. Fu B H [7] determined the spatial distribution

[1] Qinjun Wang, male, born 1975, Associate Professor. His focus is on the remote sensing of geological hazards and mineral prospecting.

of surface ruptures based on the detailed interpretation of coseismal surface ruptures using post-earthquake high-resolution remote sensing imagery. Wang X Y [8] studied the characteristics of landslides induced by the MS 8.0 Wenchuan earthquake and showed that landslides triggered by the earthquake were obviously affected by faults and distributed asymmetrically on the two sides of the Longmenshan fault. Zhu B Q [9] discussed the rule of hazard classification and analysed two programs based on different remote sensing data sources. Zhao X [10] analysed the extraction method of landslide and debris flow information based on optical remote sensing data and SAR data. Han J L [11] studied geological hazards triggered by the Wenchuan earthquake and showed that the peak ground acceleration was the strongest influencing parameter, while the secondary parameters were topography, bedrock geology, and geomorphology. Fan J R [12] investigated "dammed lakes" induced by the Wenchuan earthquake and the results showed that there were 37 dammed lakes in the main disaster area and their distribution was consistent with the earthquake fault zones.

In this study, a semi-automatic method for geological hazard extraction using high-resolution remote sensing was developed.

2. Method

A flow chart of the method for geological hazard extraction using high-resolution remote sensing imagery is shown in Figure 1. A high-resolution Digital Elevation Model (DEM) was used to create mask imagery by taking the low elevation as input conditions, and the mask imagery was used to remove interfering factors at low altitudes such as buildings, water, and bridges. Then, the mask imagery was diced into several small parts to reduce inconsistencies, and they were used as sources to be classified using unsupervised methods. After that, vector conversion was performed on the classified images to form vectors in ArcGIS. Finally, many interfering factors such as bare land, vegetation under shadows, and buildings at higher altitudes were removed from the map. It was very difficult to define one or more rules to delete them automatically, and in this case, it was more convenient to delete them manually. Following the above steps, a geological hazard map was made in ArcGIS.

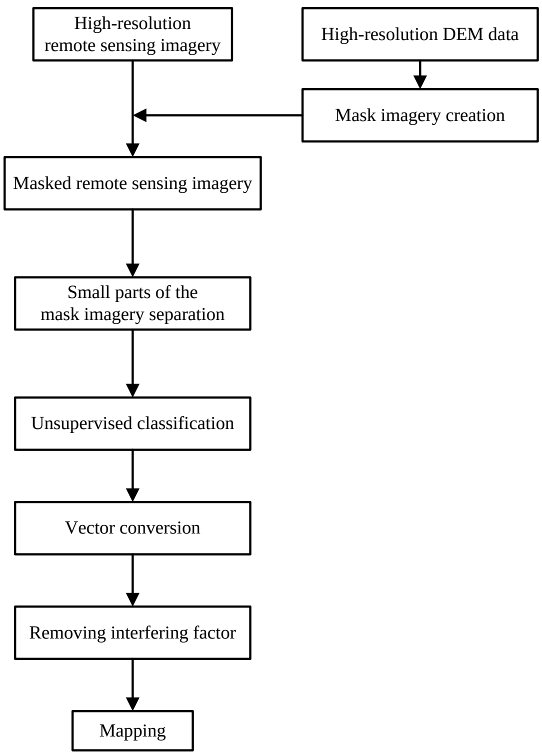

Figure 1. Flow chart of the geological hazard extraction.

3. Application

3.1. Study area

As shown in Figure 2, the town of Yingxiu is located in southeastern Wenchuan County. With a longitude of 103°26′ – 103°31′E and latitude of 31°2′ – 31°9′N, it is an important transport hub between Aba Zhou and Chengdu. Because the distance to Chengdu is just 70 km, it is the nearest town to Chengdu in Aba Zhou and the only way to Jiuzhaigou, Wolong, and Siguniangshan. With complex geological structures, the study area is located at the Longmenshan fault zone, in which the lowest altitude is 698 m and the highest is 2,396 m. With steep topography and great height differences, the topography provides favourable conditions for aggregating water on a large scale and providing great kinetic energy for loose detritus.

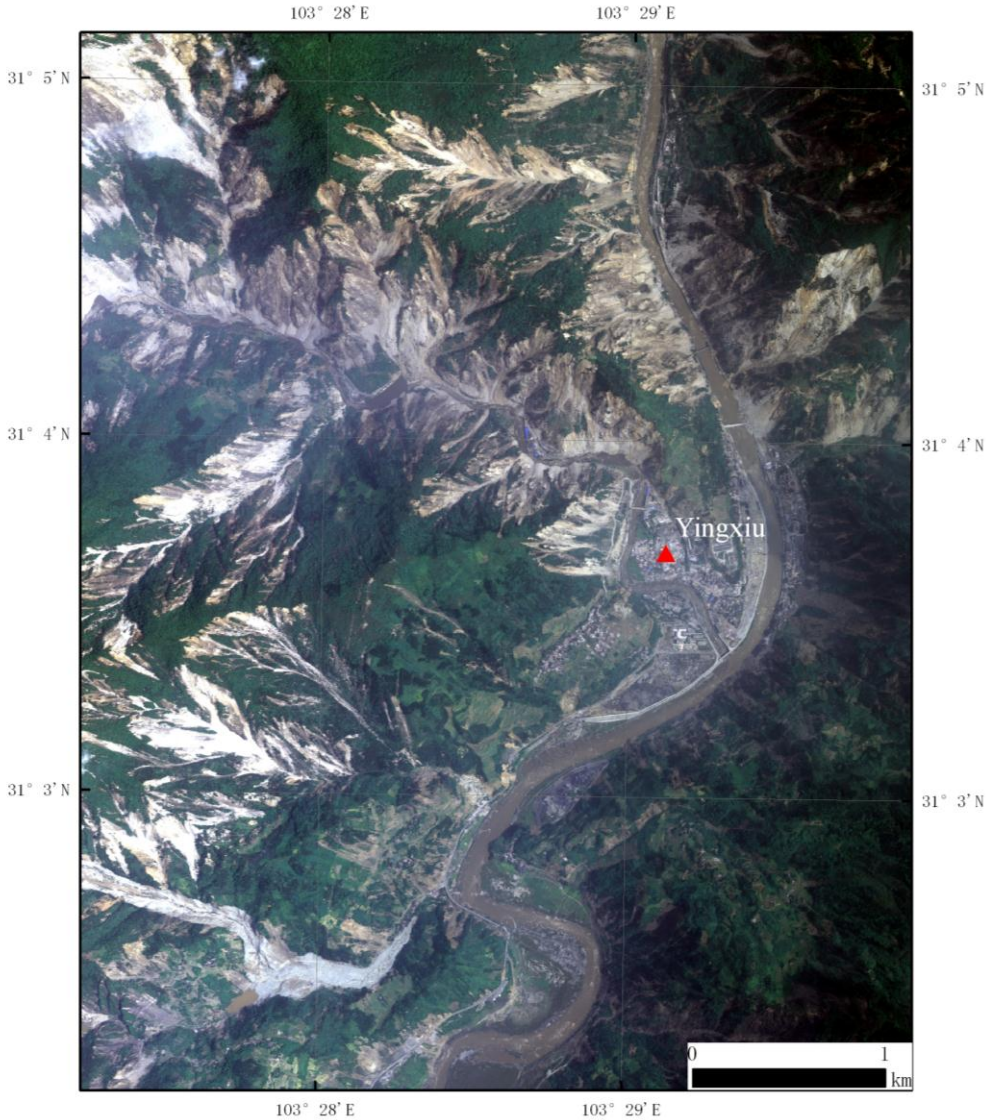

Figure 2. Original image of Yingxiu.

On May 12th, 2008, the Wenchuan earthquake struck with a magnitude of MS 8.0, and the epicentre was Yingxiu with a focal depth of 14 km. The geological environment of Yingxiu was seriously damaged by the earthquake. The ground fissures were widespread and the mixture of rocks and soils were damaged seriously to form many landslides, landslips, and debris flows. These geological hazards were extracted from high-resolution remote sensing imagery using the method presented in Section 2.

3.2. Data and processing

With a spatial resolution of 2 m, airborne remote sensing data acquired on May 15th, 2008, was used to extract geological hazards. It was composed of three bands representing red, green, and blue. There was thin fog throughout the image and thin clouds in the northwest. Fortunately, they had little influence on the geological hazard extraction. The DEM data with a spatial resolution of 0.5 m acquired on the same day was used to build mask images. With the lowest altitude being 698 m and the highest 2,396 m, it was composed of just one band.

The remote sensing imagery and the DEM imagery were then registered by selecting typical control points in the ENVI v4.5 software.

3.3. Geological hazard extraction

(1) Geological hazard identification marks

The types of geological hazards in the study area were mainly debris flows and landslides. Because the study area was mainly covered by vegetation before the earthquake, the geological hazards in the image were shown to be bright-white and grey, which is different from the green colour of the vegetation and the black-grey colour of the water in the Minjiang River.

(2) Removing interfering factors

Buildings, especially collapsed buildings, in low-altitude valleys had the same colour as geological hazards and could be removed using mask imagery built from the DEM data. Based on the statistics on the altitude of water and most buildings, the threshold to eliminate buildings was defined. At the same time, the threshold to eliminate the thin clouds was also determined based on the statistics. Then, the mask imagery was made according to the above two thresholds and was applied on the remote sensing imagery to eliminate the buildings and thin clouds.

(3) Unsupervised classification

According to the number of features on the surface, ten classes were determined to classify the imagery using the K-means unsupervised classification method in ENVI v4.5. The results of the classification were converted from raster into vectors in ArcGIS v10.0.

(4) Selected geological hazards map

Based on the classification results, the geological hazards were picked out from the vectors by their numbers and a map with a few incorrectly classified features was generated in ArcGIS.

(5) Removing incorrectly classified features

Although the main interfering factors such as buildings and water were removed using the mask imagery in the second step, there were also some incorrectly classified features such as bare lands, lands covered by sparse vegetation, and buildings at high altitudes, which were difficult to eliminate automatically. In this case, it was more efficient to remove them manually than to use the time to construct interfering factor removal rules.

(6) Mapping

After removing the interfering factors and incorrectly classified features, a geological hazard map was made in ArcGIS (Figure 3).

According to the geological hazards map, the characteristics of geological hazards were identified as follows:

(1) The geological hazards were mainly distributed along the Longmenshan structure.

As the energy released by the earthquake was mainly along the active faults, the degree of damage from geological hazards was consistent with the faults' activity, depth, and scale. Therefore, the appearance of geological hazards was closely related to the Longmenshan structure.

(2) The scale and quantity of the geological hazards are positively correlated to the energy released by the earthquake.

In the study area, the more energy the earthquake released, the more intensive the geological hazards appeared. In the strongly affected seismic areas, the distribution of geological hazards was mainly controlled by the earthquake, while traditional impact factors such as rocks, slopes, and elevation were minor.

(3) The geological hazards are linearly distributed along the valley.

Because the topography is strongly cut by the river, the elevation difference of the topography is up to 1,000 m in some areas. Steep slopes provide good conditions for geological hazards to occur. Along the valley, especially in the areas of poor rock strength, the amount of geological hazards was more than the areas with good rock strength.

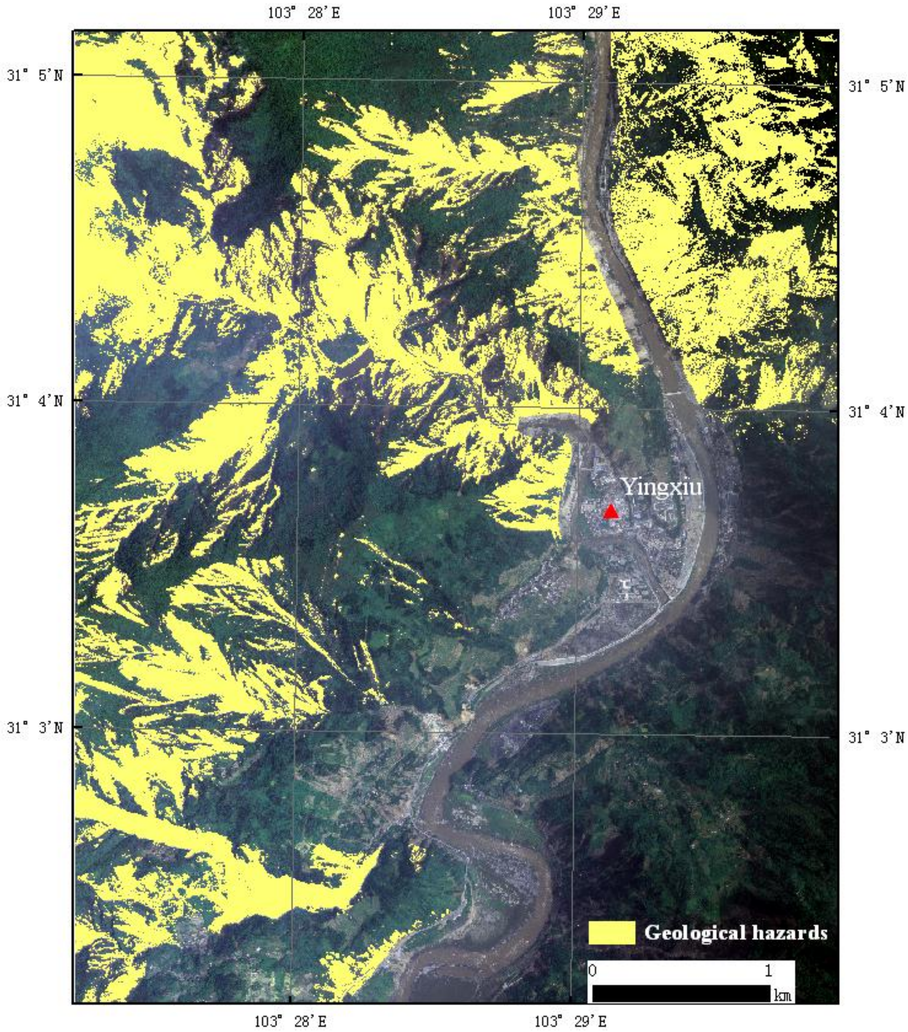

Figure 3. Geological hazards map

4. Discussion and conclusions

(1) A semi-automatic method for geological hazard extraction was proposed.

Due to the complex composition, colour, and multiple influencing factors of the geological hazards, it is difficult for researchers to automatically extract them from high-resolution remote sensing imagery. In this study, a semi-automatic geological hazard extraction method was proposed. It is helpful for researchers to improve efficiency in geological hazard mapping using remote sensing imagery and GIS software. In an emergency, the method can extract geological hazards in a short time. It is of great importance for decision-makers and rescuers who need to know the degree of damage in the disaster area, especially within 72 hours after the earthquake. Therefore, the method proposed plays an important role in making decisions, rescure, and disaster response planning.

(2) The earthquake was the main factor controlling the distribution of geological hazards.

Because of strong vibration and terrain amplification effects on slopes in the large earthquake, the slope was firstly shattered, flaccid, and disintegrated [13]. The large landslide sliding surface developed with significantly tensional characteristics, which were indicated by the steep posterior wall at the back and the gentle cut surface at the bottom. Because of the strong motivation and steep slope, the landslide substances were shown to be completely collapsed. Results of the investigation showed that high initial velocity and debris-flow and air-cushion effects were the main factors leading to the landslides to move a long distance at a high velocity. The phenomenon that geological hazards were mainly distributed along the Longmenshan structure showed that the large earthquake was the main factor controlling the distribution of geological hazards, while the traditional factors such as rocks, slopes, and elevation were minor.

(3) There is a long way for researchers to go in automatically extracting geological hazards using high-resolution remote sensing.

Because of the complexity and heterogeneity of the geological hazards' compositions, their hue and texture in the remote sensing imagery were shown to be unevenly colourful, which made accurate classification very difficult at a large scale. Furthermore, there were also such influencing factors as shadows, bare lands, and buildings affecting the classification accuracy. It is not possible to reduce them by just constructing a rule; one rule constructed for an image cannot be used completely by others. In generally, time spent in constructing a common rule to reduce the negative effect of the interfering factors cost more time than removing them manually. Therefore, there is much more work to be done to automatically extract geological hazards from high-resolution remote sensing images. Object-oriented techniques and corresponding software are needed in the future.

5. References

[1] Wei C J, Liu Y L ,Wang S X, Zhang L F and Huang X X 2008 *J. Remo. Sens.* **12(5)** 673–682
[2] Xu C, Dai FC, Chen J and Tu X B 2009 *J. Remo. Sens.* **13(4)** 754–762
[3] Chen W K, He S L, Zhang J F, Zhou Z H and Guo X N 2008 *Northw. Seis. J.* **30(1)** 88–93
[4] Wang X Q, Wei C J and Miao C G 2003 *Earth Sci. Front.* **10** 285–291
[5] Wang, X Q, Wang L, Zhang X H and Ding X 2009 *Earthquake* **29(1)** 174–181
[6] Cai S, Zhang J F and Chen W K 2009, *J. Geodesy and Geodyn.* **29(1)** 31–35
[7] Fu B H, Shi P L and Zhang Z W 2008 *Acta. Geolo. Gica. Sinica.* **82(12)** 1679–1687
[8] Wang X Y and Nie G Z 2009 *Chin. J. Geot. Engi.* **31(9)** 1378–1383
[9] Zhu B Q, Wei C J and Zhang Y Z 1998 *J. Natu. Disa.* **7(1)** 34–39
[10] Zhao X, Li C C, Su N 2009 *J. Natu. Disa.* **18(6)** 29–32
[11] Han J L, Wu S R and He S J 2009 *Earth Sci. Front.* **16(3)** 306–326
[12] Fan J R, Tian B W and Cheng G W 2008 *J. Mount. Sci.* **26(3)** 257–262
[13] Huang R Q. 2009 *Chin. J. Rock Mech. and Engi.* **28(6)** 1239–1249

Acknowledgments

This research was financially supported by the National Science and Technology Support Program (No. 2012BAK15B05), National Natural Science Foundation of China (No. 41171280), and the National Science and Technology Support Program (No. 2012BAH27B05).